Journal of Chemical Health Risks

www.jchr.org

JCHR (2025) 15(3), 2179-2188 | ISSN:2251-6727

Synthesis and Characterization of Cobalt Oxide nanoparticles by Electrochemical Reduction Method and Screening of their Antioxidant Activity

Meena B. Lande[a,b], Suresh T. Gaikwad[a] and Anjali S. Rajbhoj[a*]

a. Department of Chemistry, Dr. Babasaheb Ambedkar Marathwada University, Dist. Chhatrapati Sambhajinagar, Maharashtra, India.

b. Department of Chemistry, MES's, Arts, Commerce and Science College Sonai, Tal. Newasa, Dist. Ahmednagar, Maharashtra, India.

(Received: 16 March 2025 Revised: 20 April 2025 Accepted: 15 June 2025)

KEYWORDS

Electrochemical reduction process, Cobalt oxide, Antioxidant activity, Spectrophotometer, DPPH test.

ABSTRACT:

The nanostructured cobalt oxides (Co_3O_4) were synthesized via the electrochemical reduction process by optimizing current density at 14 mA/cm2, CTAB was used as a structure directing agent in an organic medium consisting of acetonitrile and tetrahydrofuran in a 4:1 ratio. The synthesized cobalt oxide nanoparticles were characterized by using UV-visible spectroscopy, FTIR, XRD, SEM, EDS and TEM analysis techniques. The FTIR spectra shows strong absorption peaks at 520.78 and 653.87 cm-1 verified the existence of Co_3O_4 nanoparticles. The peak observed at 294 nm in UV spectrum confirms the nanoparticles were synthesized. The X-ray diffraction (XRD) pattern shows face centered cubic spinel structure (FCC) of the Co_3O_4 nanoparticles. Scanning electron microscopy investigation showed spherical and Quasi-spherical shape surface morphology of nanoparticles. The cobalt oxide nanoparticles particle size was 37.17 nm measured using transmission electron microscopy. Energy dispersive spectroscopy was used to determine the presence of the elements Co and O. The antioxidant activity of the synthesized nanoparticles was investigated spectrophotometrically using a modified 2,2-diphenyl-1-picryl-hydrazyl (DPPH) test. The results demonstrate that synthesized Co_3O_4 nanoparticles shows 70.89 % free radical scavenging within 60min and it can be suggesting their possible applications in pharmaceutical and food industries due to its high efficiency and low cost.

1. Introduction

Over the past few decades, nanotechnology has been more and more well-liked as a promising technical development. This type of nanotechnology creates and uses materials with special properties by manipulating atoms, molecules, or macromolecules that range in size from 1 to 100 nm. Compared to bigger particles, nanoparticles have various advantages, such as an increased surface-to-volume ratio and enhanced magnetic characteristics[1]. Applications of nanotechnology can be found in physiology and medicine. This technique allows materials and devices to interact with cells and tissues at the level of molecules with a significant amount of functional specificity, enabling a level of technology and biological system integration that was previously unattainable. It should be understood that nanotechnology is not a single, new scientific field in and of itself, but rather the result of the convergence of several traditional sciences, including physics, biology, chemistry and material science, in order to gather the necessary collective expertise for the development of these cutting-edge technologies [2].

Free radicals are produced as byproducts of the metabolic processes. These extremely reactive species interact harmfully with a wide range of biomolecules. This causes a wide range of harmful illnesses in humans, including arthritis, cancer, cardiovascular disease, and diseases of the central nervous system. Although the body has its own defensive system against these free radicals, additional antioxidants are still necessary.

Journal of Chemical Health Risks
www.jchr.org
JCHR (2025) 15(3), 2179-2188 | ISSN:2251-6727

When combined with nutritional antioxidants, synthetic antioxidants may help in the prevention of certain illnesses. Numerous in vitro techniques are available for evaluating antioxidant properties, including superoxide scavenging activity, nitric oxide, hydroxyl radical, peroxynitrite, hydrogen peroxide, and nitric oxide, DPPH assay, etc. Moreover, the DPPH method is more affordable, quick, and easy to use than the other techniques. Studies on nanoparticles have focused on their potential uses as antioxidants, photoelectric, antibacterial, anticancer, and catalytic agents. According to a scan of the literature, metal oxides such as Fe_2O [3], Al_2O_3, NiO[4], and CuO[5] nanoparticles have 32–85% antioxidant activity in the DPPH test.

Typical transition metal oxides, cobalt oxide nanoparticles have intriguing catalytic characteristics and are magnetic p-type semiconductors[6]. The three main forms of cobalt-based nanoparticles in various oxidation states are cobaltous oxide (CoO), cobaltic oxide (Co_2O_3), and cobaltosic oxide (Co_3O_4) respectively[7]. Nanotechnology is highly interested in cobalt-based nanostructures because of their unique chemical and physical characteristics [8]. In the field of technology, cobalt oxide is one of the most important oxides of transition metals. Numerous techniques, including coprecipitation [9], sol–gel [10], Microwave combustion method [11], simple thermal decomposition [12] , green synthesis[13] , and electrochemical processes [14] can be used to prepared cobalt oxide nanoparticles. The unique and significant uses of Co_3O_4-NPs have garnered a lot of interest recently. These nanoparticles are used in lithium ion batteries, gas sensors, energy storage systems, solar selective absorbers, field emission materials, capacitors, electrochromic thin films, magneto resistive devices, and catalysis [16, 19-24]. Additionally, Metal oxide nanoparticles have been found to possess antibacterial, Antifungal and Antioxidant properties not just because of the release of metal ions in solution, but also because of their high surface to volume ratio and tiny size, which enable them to adhere tightly to the membranes of microbes [15].

In the present work, we modified the electrochemical reduction approach to synthesize cobalt oxide nanoparticles by electrolyzing them with a regulated current. The CTAB salts, which are very soluble and separate in the solvent to function as an electrolyte and a capping agent, were utilized. Also, the antioxidant activity of these nanoparticles was investigated. The free radical scavenging assay [DPPH assay] was used for evaluating the antioxidant activity of Co_3O_4 nanoparticles at different Co_3O_4 concentrations and time intervals.

2.Materials and Methods

2.1 Materials

All compounds were purchased from Sigma Aldrich and Rankem chemical suppliers (purity up to 98.99%) and used as received. The HPLC grade cetyl trimethyl ammonium bromide salts (CTAB), acetonitrile (ACN) and tetrahydrofuran (THF) were purchased from Rankem chemicals. Alfa Aesar provided the sacrificial anode in the form of cobalt sheet and platinum sheets as an inert cathode with a thickness of 0.5 mm and a purity of 99.99%.

2.2 Synthesis of Cobalt oxide nanoparticles

The electrochemical approach can be used to create pure and size-selective nanoparticles. The method uses a low-cost two electrode setup for a 25–30 ml electrolyte solution, and it combines the reduction of metal ions with the oxidation of bulk metal to generate size-selective tetra alkyl ammonium salt stabilized metal nanoparticles. A 1x1 cm sheet of cobalt metal was used as the anode and a 1x1 cm sheet of platinum was utilized as the cathode in the experiment. The supporting electrolyte for these two electrodes was 0.01 M solutions of cetyl trimethyl ammonium bromide salt (CTAB) prepared in THF/ACN (1:4). The two electrodes were placed 1 cm apart from one other as shown in Fig.1. After that, the electrolysis process was run for 2 hrs at a current density of 14 mA/cm^2. Electrolysis was performed in nitrogen atmosphere. Cobalt oxide nanoparticles have been observed black in color. After electrolysis, the nanoparticles were allowed to settle at least one day. Decantation was used to separate the solid material from the solution, and THF was used to wash it three or four times to remove excess CTAB. Following washing, the samples were dried in vacuum desiccators, calcined at 350^{o}C, and used for characterizations.

Mechanism of synthesis of Cobalt oxide nanoparticles

During the synthesis process, the bulk metal anode is oxidized and converted into metal cations. These cations

Journal of Chemical Health Risks
www.jchr.org
JCHR (2025) 15(3), 2179-2188 | ISSN:2251-6727

travel to the cathode, where reduction takes place and metal with zero oxidation is created.

Anode – M^0 bulk→ M^{n+} + ne$^-$

Cathode -M^{n+} + ne$^-$ + stabilizer →M^0 coll / Stabilizer

M^0 bulk + stabilizer →M^0 coll / stabilizer

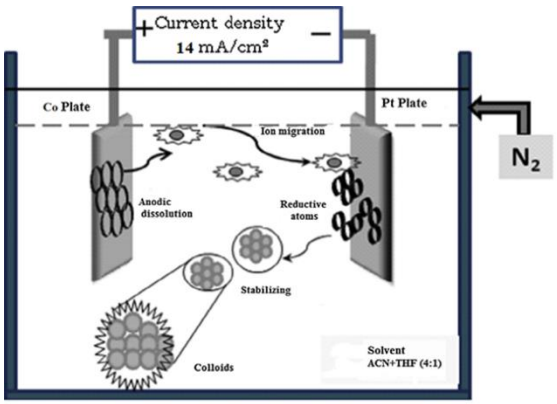

Fig. 1 Diagram representing the synthesis process of Cobalt oxide nanoparticles

2.3 Antioxidant Activity

A modified DPPH method, as described by Serpen et al. [16], was implemented requiring little modifications since the metal oxide nanoparticles are insoluble in methanol. A reaction vial containing 100 mg of powdered nanoparticles and 3 ml (100 µM) of DPPH methanolic solution was filled. The radical source utilized in this experiment was DPPH, while the radical scavenger was nanoparticles. When the DPPH radical is in solution, it is dark violet in color; however, when nanoparticles are present, it eventually turns light yellow or colorless. The mixture was further sonicated and held in the dark to speed up the pace of interaction between the nanoparticles and the DPPH reagent. For five minutes, the contents were centrifuged at 10,000 rpm. The wavelength scan for the supernatant was done from 400 to 700 nm (scan rate 1.00 mm/s) since DPPH has an absorption peak at 517 nm. The DPPH control used as a reference.

The above process was repeated to investigate the time-dependent DPPH scavenging at intervals of 5, 15, 30, 45, and 60 minutes. The formula was used to determine the percentage of DPPH radical scavenging.

$$\% \text{ DPPH Scavenging} = [1 - As/Ac] \times 100$$

Where, A_C and A_S are Absorbance of DPPH (Control) and supernatant DPPH Solvent respectively. Using the above described method, the SC 50 (amount needed to scavenge 50% DPPH) value was determined for various nanoparticle quantities, ranging from 20 mg to 100 mg, and absorbances were recorded after 30 minutes

3.Result and Discussion

3.1 Characterization Techniques:

Structural studies of the synthesized cobalt oxide material were done by using UV–Visible spectrophotometry, FTIR, XRD, TEM, SEM–EDS techniques. The resulting solid nanoclusters were mixed with KBr, and FTIR spectra in the 400–4000 cm^{-1} range were recorded using the Jasco FTIR 8400 Spectrophotometer. The supernatant of generated nanoparticles was used in UV-visible spectroscopic examination for surface Plasmon absorption in the UV-visible region and color recording using Jasco UV-visible spectroscopy.

Using Cu Kα radiation (λ = 1.54 A °), the powdered X-ray diffraction patterns were acquired on the Rigaku X-ray diffractometer (Ultima IV). Scanning electron micrograph (JEOL 6390LA) was used to examine the morphology of the produced nanoparticles. An energy dispersive spectrophotometer (EDS) was used to investigate the existence and elemental composition of nanoparticles. Transmission electron microscopy was used to examine the produced nanoclusters. The TEM analysis was performed by using JEM 2100 TEM at 200 kv.

3.2 Fourier Transform Infra-red Studies (FTIR):

Fourier transform infrared spectroscopy was used to study the chemical bonding information of the cobalt oxide nanoparticles, and Fig.2 illustrates the features of the IR bands displayed in the 4000-400 cm^{-1} region**.** The quality and composition of metal or metal oxide nanoparticles were determined using FTIR spectroscopy. The occurrence of Co_3O_4 nanoparticles is confirmed by the FTIR spectra, which revealed strong absorption peaks at 520.78 and 653.87 cm^{-1} that are related to the finger print stretching vibrational modes of cobalt-oxygen (Co-O) bonds, which supports the presence of phase purity with monodispersed in the face centered cubic structure [17]. The Co-O stretching vibration

Journal of Chemical Health Risks
www.jchr.org
JCHR (2025) 15(3), 2179-2188 | ISSN:2251-6727

mode, which is represented by the absorption band at 520.78 cm^{-1}, indicates the presence of Co^{3+} ions in the octahedral site. The crystal lattice structure's type ABO_3 (where A denotes the Co^{2+} in the tetrahedral site) bridging vibration of the O-Co-O bond, designated at 653.87 cm^{-1}, indicating the $Co^{2+}Co^{3+}O_3$ bonding vibrations.

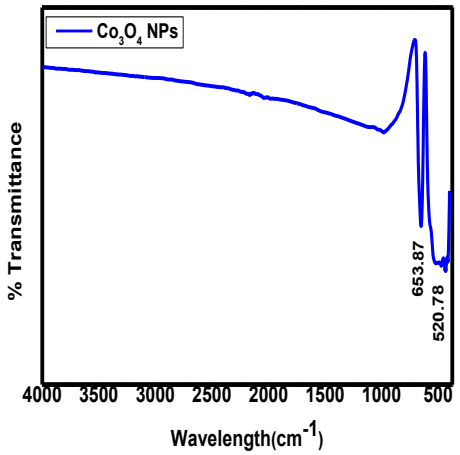

Fig.2 FTIR Spectra of Cobalt oxide nanoparticles with CTAB at current density 14 mA/cm²

3.3 UV–Visible Spectroscopic Analysis

The color changes that accompanied the reduction of cobalt ions made it visually apparent. It is only after calcinations that the CTAB encapsulating these cobalt oxide nanoparticles is totally eliminated. The electrochemical mechanism, which is dependent on current density, controls the diffusion of the generation of nanoparticles and is dependent on the concentration of ions at the electrode surface and in the bulk. The UV–visible spectrum of the Cobalt oxide nanoparticles is presented in Fig. 3. Generally, electronic transitions are examined in the spectrum region. Since metal oxide nanoparticles have quantum size effects, their UV-visible spectra usually have a long tail that extends towards the longer wavelength. Upon recording the UV-visible spectra of cobalt oxide nanoparticles, a similar phenomenon was observed. The UV spectrum is a peak observed at 296 nm, which confirms the nanoparticles was synthesized.

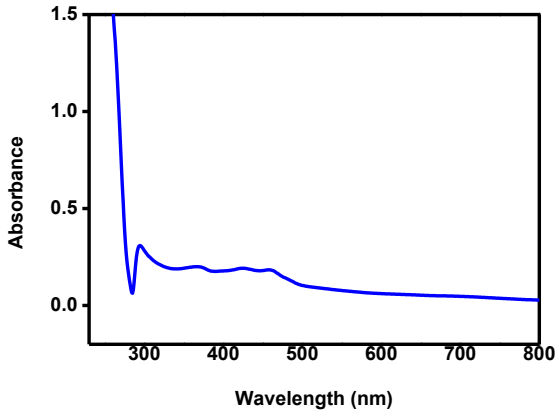

Fig.3 UV-Visible Spectrum of Cobalt Oxide Nanoparticles

3.4 X- ray diffraction (XRD)

Using XRD, the synthesized Cobalt oxide nanoparticles phase confirmation was done. The bulk average size of coherently diffracting domains may be found via X-ray line broadening analysis. The sample of cobalt oxide nanoparticle conducted X-ray diffraction (XRD) testing to confirm the predicted crystal structure and calculate average grain sizes. Using the Debye–Scherrer's equation, one may infer the average crystallite size (D) of a solid material from X-ray line broadening.

$$D = \frac{k\lambda}{\beta \cos\theta}$$

In the equation, D is Average particle size (nm); k is Scherrer constant, which typically takes a value of 0.98; λ is the X-ray wavelength; θ is diffraction angles; β is Full width at half maximum (FWHM).

Particle Size Studies:

X-ray diffraction (XRD) pattern of the synthesized cobalt oxide nanoparticles demonstrates the crystalline nature, phase purity and structure details. Fig.4 shows the powder XRD pattern recorded for as prepared cobalt oxide (Co_3O_4) nanoparticles. The sharp peaks indicate the great crystallinity of the prepared material with no peaks of other phases or impurities observed. The powder X-ray diffraction (XRD) with Cu Kα radiation (λ= 1.54 A °) radiation. Five diffraction peaks (220), (311), (400), (511), and (440) were observed. Their peak

Journal of Chemical Health Risks
www.jchr.org
JCHR (2025) 15(3), 2179-2188 | ISSN:2251-6727

position and their intensity also match the standard pattern of Face Centered Cubic (FCC) type (Joint Committee on Powder Diffraction Standards (JCPDS) file no. 80-1541) [43]. The 2θ values for the plane's peaks (220), (311), (400), (511), and (440) were found to be 31.32, 36.92, 44.80, 59.41,65.28 respectively.

The XRD pattern shows face centered cubic spinel structure (FCC) in the sample with a space group Fd3m, in which the Co^{2+} occupies the tetrahedral and the Co^{3+} occupies the octahedral sites, is indexed to the observed planes. The well-defined peaks signify the elevated crystallinity of the analyzed sample, absent of any other peaks related to other phases or contaminants. Bragg's law is used to determine the lattice constant. The lattice constant is a = b = c was 8.083A°, matched with JCPDS file no. 80-1541 as shown in Fig.4. Since the peak from the most intense plane diffraction was selected to calculate the average particle size, it was found to be 38.58 nm. This value correlates with the TEM results.

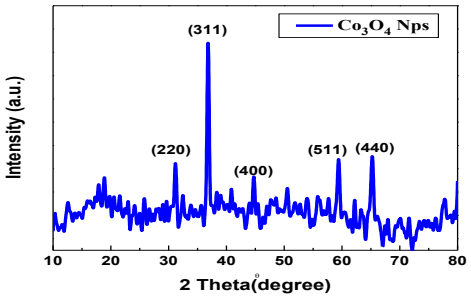

Fig.4 Shows X-ray diffraction pattern of cobalt oxide nanoparticles with CTAB at 14 mA/cm^2

3.5 Scanning electron microscopy (SEM)

The nanoscale particle morphology was obtained using the scanning electron microscopy (SEM) imaging method. The SEM picture demonstrates spherical and Quasi-spherical structures of Cobalt oxide nanoparticles shown in Fig 5(a) and (b). SEM gives information on the homogeneity, size distribution, and size of nanoparticles. The SEM image shows a homogeneous distribution of particles. From SEM images Fig 5(a) and (b) shown the nanoparticles size ranges from 20-50 nm.

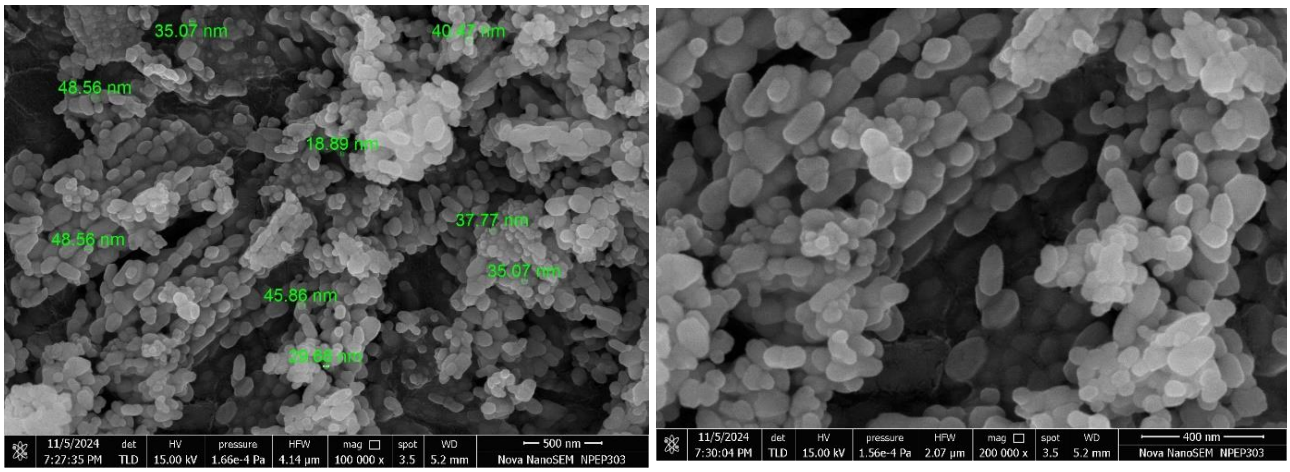

Fig.5 Shows SEM image of Cobalt oxide nanoparticles with CTAB at 14 mA/cm^2

3.6 Energy dispersive spectroscopy (EDX):

The elemental composition of Cobalt oxide NPs is determined by energy dispersive spectroscopy. An analysis using energy-dispersive spectroscopy verified the existence of cobalt oxide NPs. The illustration of the usual ED spectra can be found in Fig.6(a). The spectra of synthesized cobalt oxide NPs show four distinct peaks, which peaks correspond to cobalt and oxygen. The capping agent responsible for the partial oxidation of the nanoparticles during sample handling owing to ambient oxygen is the source of the oxygen component seen in the graph. The weight percentage of Cobalt and oxygen atoms, which was determined to be 81.92 and 18.08%, respectively, is shown in Fig.6(b). This clearly illustrates the creation of pure Co_3O_4 nanoparticles.

Journal of Chemical Health Risks
www.jchr.org
JCHR (2025) 15(3), 2179-2188 | ISSN:2251-6727

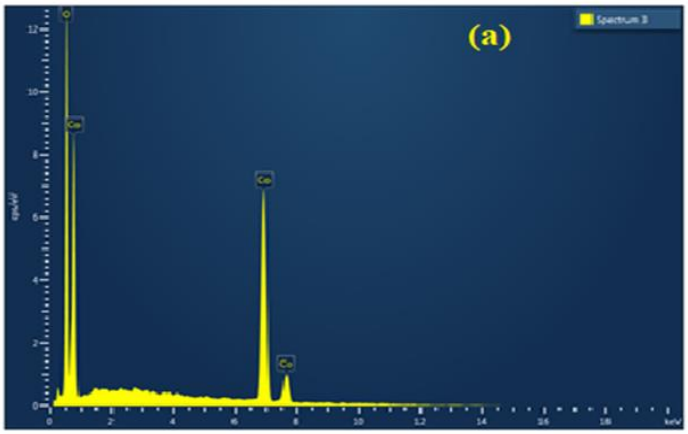

(b) Elements	Mass%	Atomic %
O	18.08	44.84
Co	81.92	55.16
Total:	100	100

Fig.6(a) EDX spectrum of Co_3O_4 nanoparticles (b) composition of Co & O element

3.7 Transmission electron microscopy (TEM)

The TEM image of cobalt oxide nanoparticles shown in Fig. 7(a) represent actual morphological observations of the particles. The majority of the particles were tiny, spherical, Quasi-pherical, and some cubic were also visible in Fig. 7(a), according to micrographs. TEM image (Figs. 7(a) and (b)) along with histogram of particle size distribution of the typical product indicated that cobalt oxide nanoparticles were dispersed and no aggregation was observed. The Gaussian fitment curves in respect of the particle size distribution have also been provided in Fig.7b. As can be seen from the figure, the size of the particles are controlled mostly within 30-50 nm. The average particle size of Co_3O_4 nanoparticles was measured to be D = 37.17 nm, which is slightly greater than that obtained from XRD analysis. This may be attributed to the stretched lattice that is clearly shows in the obtained lattice constant. Consequently, this influences peak broadening, which influences Scherrer's formula's predicted nanoparticle size.

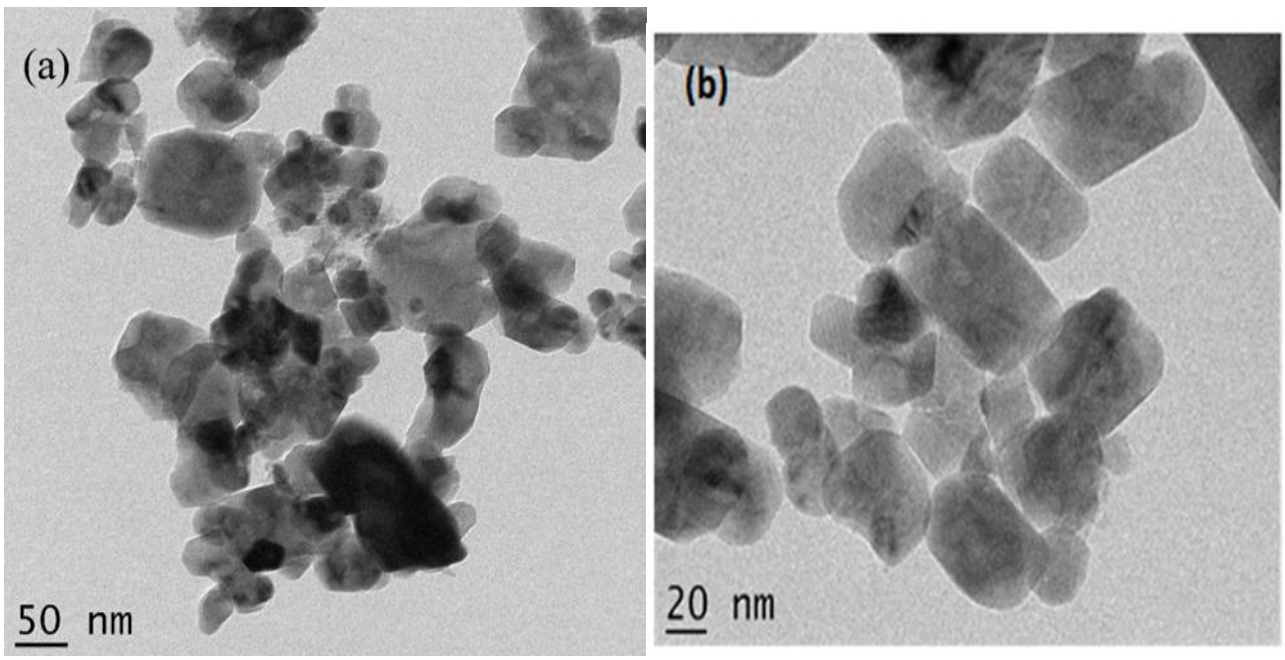

Journal of Chemical Health Risks
www.jchr.org
JCHR (2025) 15(3), 2179-2188 | ISSN:2251-6727

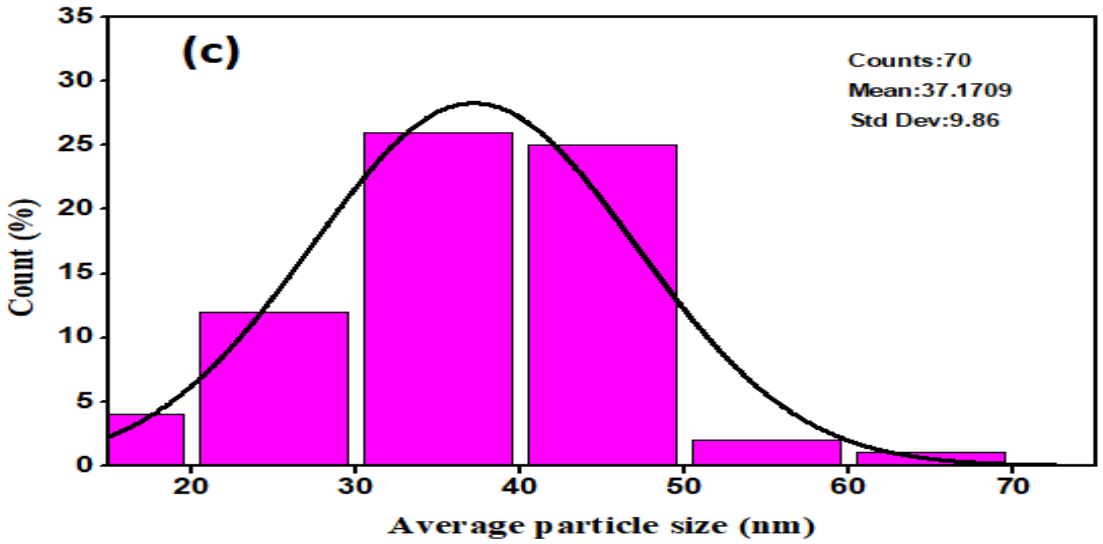

Fig. 7 (a) & (b) TEM images of cobalt oxide nanoparticles and (C) particle size histogram of nanoparticles prepared at current density 14 mA/cm^2

3.8 Selected Area Electron Diffraction (SAED) Pattern

Electron diffraction data was gathered to determine phases of cobalt oxide nanoparticles. The electron diffraction pattern of the chosen nanoparticle region is displayed in Fig.8. Regarding the Co_3O_4 nanoparticles, the SAED pattern verified the cubic structure, which was consistent with the XRD data mentioned earlier. The outcome showed that the particular region of grain boundaries was unquestionably important for the ferromagnetic characteristics of Co_3O_4 nanoparticles. The samples only exhibit ferromagnetic characteristics. Even if the specific area is vast and the Co_3O_4 particles are very tiny, free surfaces do not cause ferromagnetism if the sample's grain boundaries are missing.

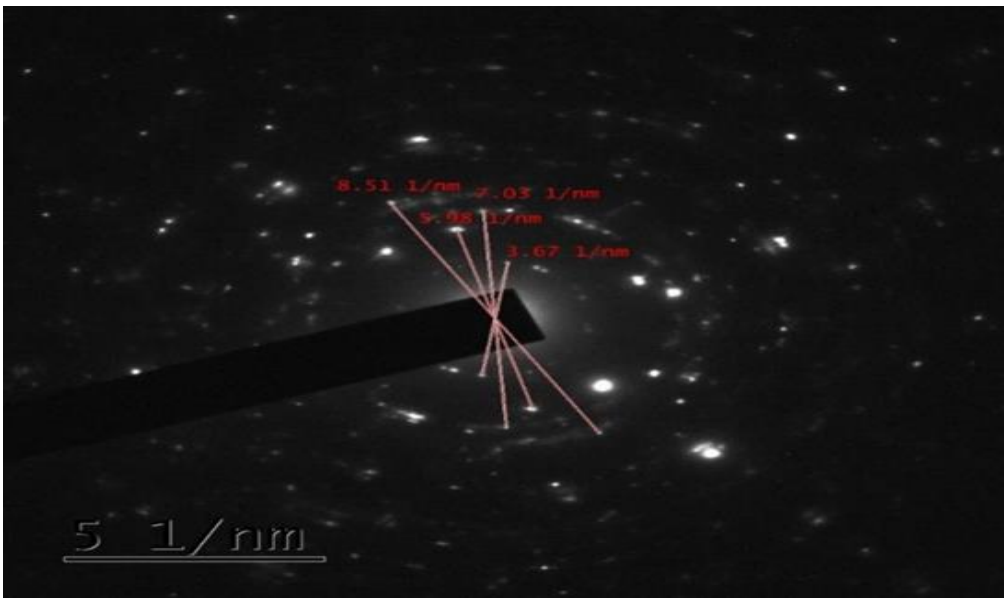

Fig.8 SAED pattern of Cobalt Oxide Nanoparticles

Journal of Chemical Health Risks
www.jchr.org
JCHR (2025) 15(3), 2179-2188 | ISSN:2251-6727

3.9 DPPH radical Scavenging Activity

The antioxidant effectiveness of cobalt oxide NPs can be attributed to the time-dependent quenching of the DPPH free radical, as shown in Fig. 9(a), since the control (DPPH without NPs) exhibits no change in absorption peak with time. The quantity of DPPH in the methanolic solution can be determined by the decrease in absorbance at 517 nm, which can be used to determine the percentage of DPPH scavenging. It is evident from Fig.9(a) that time t=30 min and t=60 min, more than 37.11 and 70.89% of DPPH respectively got scavenged. The SC 50 value was found to be 60.52 mg which was obtained by graphical analysis shown in Fig.9(c). The observed beneficial antioxidant activity may result from the process of an electron being transferred between the reactants, which neutralizes the free radical nature of DPPH.

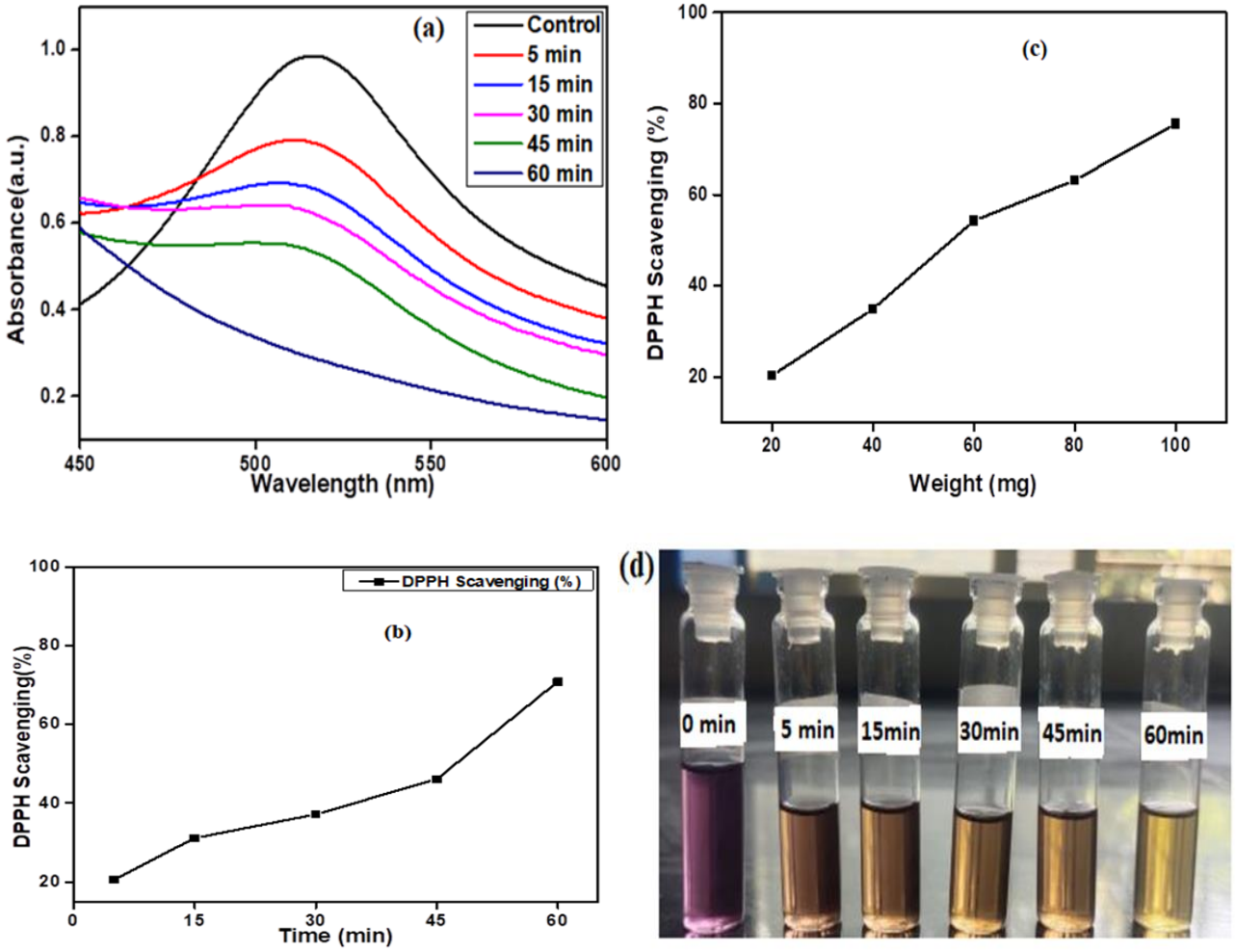

Fig.9 Antioxidant Activity:(a) and (b)Time dependent free radical scavenging by Co_3O_4 NPs (c) DPPH scavenging (%) at different amount of Co_3O_4 NPs (c) Visual Inspection of color changes of DPPH with varies time from 0 min to 60 min

Mechanism of Antioxidant Activity of cobalt oxide Nanoparticles

DPPH• is a π-radical that exists in both solid and solution states in its monomer form. According to the first structural data, extensive conjugation had less of an impact on the molecule's unusually low reactivity than "efficient screening within the hydrazyl structure of the surrounding parts". The radical is soluble in different organic solvents. It is dissolved in methanol.

Journal of Chemical Health Risks
www.jchr.org
JCHR (2025) 15(3), 2179-2188 | ISSN:2251-6727

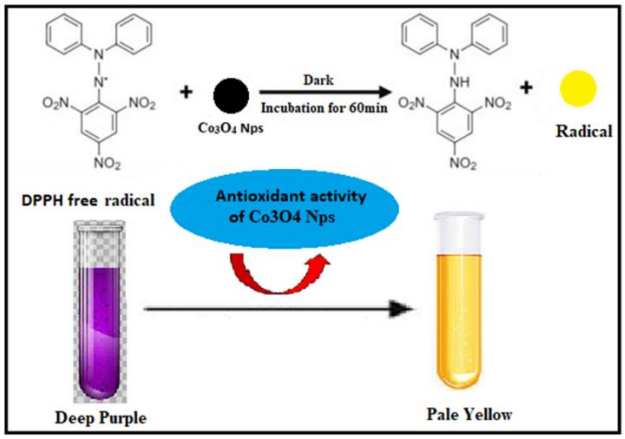

Fig.10 Mechanism of Antioxidant Activity of Co_3O_4 Nanoparticles

The neutralization step in the DPPH test depends on the antioxidants' ability to donate electrons to neutralize the DPPH radical. Co_3O_4 Nps smaller size is thought to be responsible for their antioxidant activity, but there's also a possibility that it's related to a phenomenon in 2,2-diphenyl-1-picrylhydrazyl (DPPH), where electron density is transferred from the oxygen atom to the odd electron at the nitrogen atom, causing the intensity of the $n \rightarrow \pi^*$ transition at 517 nm to decrease. The mechanism of the antioxidant activity involves the unstable deep violet-colored methanolic solution of DPPH, which, upon the addition of Co_3O_4 NPs, and paced in dark for incubation turns into a stable pale-yellow color due to their ability to scavenge free radicals containing DPPH by transferring an electron from an oxygen atom to an odd electron of a nitrogen atom, resulting in the formation of a stable DPPH molecule (Fig.10)

4. CONCLUSION

Cobalt oxide nanoparticles have been effectively synthesized by using selected stabilizers in the electrochemical reduction process. The FTIR spectroscopic study of the Cobalt oxide nanoparticles was verified the removal of the capping agent after calcinations. The optical spectra reveal absorption peak at 294 nm which confirm the metallic nature in stabilizer. Using XRD analysis, it was determined that the Co_3O_4 nanoparticles corresponded to the FCC spinel structure and the average particle size was 38.58 nm. SEM confirms that the nanoparticles are nano size, spherical and Quasi-spherical appearance. The TEM investigations revealed that the range of particle size of Co_3O_4 nanoparticles was 20-50 nm. A scavenging free radical DPPH study of Cobalt oxide NPs was done and it revealed that in 60 min Cobalt Oxide show 70.89 % free radical scavenging. Thus, Co_3O_4 Nanoparticles are a potential antioxidant property. It is also evident from the experiment that as the concentration of Co_3O_4 nanoparticles increases, it also increases their antioxidant activity. In conclusion, after carrying out more thorough research in the future, the antioxidant potentials of Co_3O_4 nanoparticles as a synthetic antioxidant may be investigated to address the various problems of veterinary sciences, medical sciences, agriculture, food sciences, etc.

ACKNOWLEDGEMENTS

The authors are greatly thankful to Department of Chemistry, Dr. Babasaheb Ambedkar Marathwada University, Aurangabad (Chhatrapati Sambhajinagar) and Principal of Mula Education Society's Arts, Commerce and Science College Sonai, Newasa, Ahmednagar, Savitribai Phule Pune University, Pune.

References:

[1] I. Luisetto, F. Pepe, and E. Bemporad, "Preparation and characterization of nano cobalt oxide," *J. Nanoparticle Res.*, vol. 10, no. SUPPL. 1, pp. 59–67, 2008, doi: 10.1007/s11051-008-9365-4.

[2] G. A. Silva, "Introduction to nanotechnology and its applications to medicine," *Surg. Neurol.*, vol. 61, no. 3, pp. 216–220, 2004, doi: 10.1016/j.surneu.2003.09.036.

[3] S. Majeed *et al.*, "Bacteria Mediated Synthesis of Iron Oxide Nanoparticles and Their Antibacterial, Antioxidant, Cytocompatibility Properties," *J. Clust. Sci.*, vol. 32, no. 4, pp. 1083–1094, 2021, doi: 10.1007/s10876-020-01876-7.

[4] A. Chahardoli, N. Karimi, X. Ma, and F. Qalekhani, "Effects of engineered aluminum and nickel oxide nanoparticles on the growth and antioxidant defense systems of Nigella arvensis L.," *Sci. Rep.*, vol. 10, no. 1, pp. 1–11, 2020, doi: 10.1038/s41598-020-60841-6.

[5] S. Wu, S. Rajeshkumar, M. Madasamy, and V. Mahendran, "Green synthesis of copper

Journal of Chemical Health Risks

www.jchr.org

JCHR (2025) 15(3), 2179-2188 | ISSN:2251-6727

nanoparticles using Cissus vitiginea and its antioxidant and antibacterial activity against urinary tract infection pathogens," *Artif. Cells, Nanomedicine Biotechnol.*, vol. 48, no. 1, pp. 1153–1158, 2020, doi: 10.1080/21691401.2020.1817053.

[6] M. S. Samuel *et al.*, "Green synthesis of cobalt-oxide nanoparticle using jumbo Muscadine (Vitis rotundifolia): Characterization and photo-catalytic activity of acid Blue-74," *J. Photochem. Photobiol. B Biol.*, vol. 211, no. July, p. 112011, 2020, doi: 10.1016/j.jphotobiol.2020.112011.

[7] N. Akhlaghi, G. Najafpour-Darzi, and H. Younesi, "Facile and green synthesis of cobalt oxide nanoparticles using ethanolic extract of Trigonella foenumgraceum (Fenugreek) leaves," *Adv. Powder Technol.*, vol. 31, no. 8, pp. 3562–3569, 2020, doi: 10.1016/j.apt.2020.07.004.

[8] B. Morcos *et al.*, "cobalt nanoparticles synthesized in ionic liquids Grenoble Alpes , F-38000 Grenoble , France ; CEA , LETI , MINATEC Campus , Jeanne Marvig , F-31055 Toulouse , France Univ . Grenoble Alpes , F-38000 Grenoble , France ; CEA , LETI , MINATEC Campus ," 2018, doi: 10.1021/acs.langmuir.8b00271.

[9] V. Ratchagar *et al.*, "Coprecipitation Methodology Synthesis of Cobalt-Oxide Nanomaterials Influenced by pH Conditions: Opportunities in Optoelectronic Applications," *Int. J. Photoenergy*, vol. 2023, no. Cv, 2023, doi: 10.1155/2023/2493231.

[10] S. A. Al Kiey, A. A. Sery, and H. K. Farag, "Sol-gel synthesis of nanostructured cobalt oxide in four different ionic liquids," *J. Sol-Gel Sci. Technol.*, vol. 106, no. 1, pp. 37–43, 2023, doi: 10.1007/s10971-023-06040-x.

[11] S. Kanimozhi and T. Ezhilarasu, "Structural , optical and magnetic properties of cobalt oxide nanoparticles synthesized by simple combustion method," vol. 11, pp. 1491–1504, 2022.

[12] S. Farhadi, J. Safabakhsh, and P. Zaringhadam, "Synthesis , characterization , and investigation of optical and magnetic properties of cobalt oxide (Co 3 O 4) nanoparticles," 2013.

[13] O. Pardeshi and A. V Patil, "Green synthesis of cobalt oxide nanoparticles using Polyalthia longifolia leaves extract," vol. 5, no. 1, pp. 1423–1430, 2018.

[14] A. Ledo-Suárez, L. Rodríguez-Sánchez, M. C. Blanco, and M. A. López-Quintela, "Electrochemical synthesis and stabilization of cobalt nanoparticles," *Phys. Status Solidi Appl. Mater. Sci.*, vol. 203, no. 6, pp. 1234–1240, 2006, doi: 10.1002/pssa.200566196.

[15] A. Manuscript, "Green Chemistry," 2020, doi: 10.1039/D0GC00885K.

[16] A. R. D. A. S. Erpen, E. D. C. Apuano, V. I. F. Ogliano, and V. U. G. Ökmen, "A New Procedure To Measure the Antioxidant Activity of Insoluble Food Components," pp. 7676–7681, 2007.

[17] S. Haq *et al.*, "Green synthesis of cobalt oxide nanoparticles and the effect of annealing temperature on their physiochemical and biological properties," *Mater. Res. Express*, vol. 8, no. 7, 2021, doi: 10.1088/2053-1591/ac1187.